Cellular/Molecular

Sustained Neuronal Activity Generated by Glial Plasticity

Tiina M. Pirttimaki, Stephen D. Hall, and H. Rheinallt Parri
School of Life and Health Sciences, Aston University, Birmingham, B4 7ET, United Kingdom

Astrocytes release gliotransmitters, notably glutamate, that can affect neuronal and synaptic activity. In particular, astrocytic glutamate release results in the generation of NMDA receptor (NMDA-R)-mediated slow inward currents (SICs) in neurons. However, factors underlying the emergence of SICs and their physiological roles are essentially unknown. Here we show that, in acute slices of rat somatosensory thalamus, stimulation of lemniscal or cortical afferents results in a sustained increase of SICs in thalamocortical (TC) neurons that outlasts the duration of the stimulus by 1 h. This long-term enhancement of astrocytic glutamate release is induced by group I metabotropic glutamate receptors and is dependent on astrocytic intracellular calcium. Neuronal SICs are mediated by extrasynaptic NR2B subunit-containing NMDA-Rs and are capable of eliciting bursts. These are distinct from T-type Ca^{2+} channel-dependent bursts of action potentials and are synchronized in neighboring TC neurons. These findings describe a previously unrecognized form of excitatory, nonsynaptic plasticity in the CNS that feeds forward to generate local neuronal firing long after stimulus termination.

Introduction

Astrocytes are now recognized as being active partners with neurons in synaptic communication (Volterra and Meldolesi, 2005). Specifically, astrocytes sense the same synaptic inputs as neurons and respond to the released neurotransmitters with intracellular calcium ($[Ca^{2+}]_i$) elevations (Cornell-Bell et al., 1990; Porter and McCarthy, 1996; Araque et al., 2002; D'Ascenzo et al., 2007). Elevating astrocytic $[Ca^{2+}]_i$ can induce the release of gliotransmitters (GTs) such as glutamate (Pasti et al., 1997; Kang et al., 1998; Parri et al., 2001; Fellin et al., 2004; Perea and Araque, 2005), ATP (Pascual et al., 2005; Serrano et al., 2006), and D-serine (Henneberger et al., 2010). This gliotransmission affects neuronal activity and function by modulating presynaptic neurotransmitter release (Fiacco and McCarthy, 2004; Liu et al., 2004a; Jourdain et al., 2007; Perea and Araque, 2007) and postsynaptic efficacy (Oliet et al., 2001; Panatier et al., 2006). Astrocytic GT release also contributes to neuronal plasticity and synaptic potentiation (Yang et al., 2003; Pascual et al., 2005; Serrano et al., 2006; Perea and Araque, 2007; Henneberger et al., 2010). In addition, astrocytic glutamate release targeting postsynaptic NMDA receptors (NMDA-Rs) generates characteristic slow inward currents (SICs) (Parri et al., 2001; Angulo et al., 2004; Fellin et al., 2004; D'Ascenzo et al., 2007) and can induce synchronous neuronal excitation (Angulo et al., 2004; Fellin et al., 2004, 2006a; D'Ascenzo et al., 2007). Some studies using glial

targeted transgenic approaches, however, challenge the proposed physiological roles and indeed the very concept of $[Ca^{2+}]_i$-dependent GT release (Fiacco et al., 2007; Petravicz et al., 2008; Agulhon et al., 2010). These studies underline the importance of verifying experimentally the cellular identity and $[Ca^{2+}]_i$ dependence of suspected astrocytic events.

Thalamocortical (TC) neurons in the ventrobasal (VB) nucleus of the somatosensory thalamus receive persistent synaptic input from glutamatergic afferents; peripheral somatosensory input is conveyed via the medial lemniscus and cortical input via corticothalamic (CT) afferents in the awake state and, in sleep, from CT afferents (Steriade, 2006). *In vitro*, stimulation of somatosensory and CT afferents induces metabotropic glutamate receptors (mGluR)-mediated astrocytic $[Ca^{2+}]_i$ elevations in the VB thalamus (Parri et al., 2010), and, similarly, *in vivo*, whisker stimulation results in glutamate-mediated astrocytic $[Ca^{2+}]_i$ elevations in the somatosensory cortex (Wang et al., 2006). SICs recorded from TC neurons occur both spontaneously and in response to mGluR agonist activation (Parri et al., 2001). It would therefore be predicted that, in the VB thalamus, afferent activity would result in astrocytic glutamate release. However, little is known about factors that may influence astrocytic glutamate release leading to SICs or the possible physiological roles of these events.

Here, we investigated the relationship between afferent activity and astrocytic output in acute VB thalamus slice preparations. We found that repetitive trains of lemniscal or CT afferent stimulation lead to a sustained increase in SICs in TC neurons that outlasts the duration of the stimulus by ~60 min. We propose that this long-term enhancement (LTE) of astrocytic glutamate release represents a glial "memory" of previous afferent activity with the capacity to drive neuronal output independent of continuing synaptic input.

Materials and Methods

Slice preparation. All procedures were performed in accordance with the United Kingdom Animals (Scientific Procedures) Act 1986 and associ-

ated procedures. Horizontal slices of VB thalamus were prepared as described previously (Parri et al., 2001) from 6- to 23-d-old male Wistar rats. After removal, the brain was placed in ice-cold modified artificial CSF (ACSF) containing the following (in mM): 126 NaCl, 26 NaHCO$_3$, 1 KCl, 1.25 KH$_2$PO$_4$, 5 MgSO$_4$, 1 CaCl$_2$, and 10 glucose. Slices were then maintained at room temperature (23–25°C) in this solution for a recovery period of 1 h before experimental use.

Solutions and chemicals. The standard recording ACSF used in this study contained the following (in mM): 126 NaCl, 26 NaHCO$_3$, 2.5 KCl, 1.25 KH$_2$PO$_4$, 1 MgSO$_4$, 2 CaCl$_2$, and 10 glucose, unless otherwise stated. As we (Parri et al., 2001) and others have done previously in attempting to enhance NMDA-R-mediated current detection, whole-cell voltage-clamp recordings were conducted in 0 Mg^{2+} at room temperature, unless otherwise stated. However, we found that SIC frequency and kinetic parameters were not different from those recorded in more physiological conditions (+33°C, 1 mM Mg^{2+}) (data not shown). All current-clamp recordings were conducted at +33°C in presence of 1 mM Mg^{2+}. Pharmacological compounds were included in the ACSF as stated in text. In experiments in which agonists were used to mimic the effect of synaptic input, agonist was perfused over the brain slice in the recording chamber for ≥1 h. Agonist was washed off before SIC recording. Chemicals were obtained from Sigma unless otherwise stated. 2-Chloro-5-hydroxyphenylglycine (CHPG), (*RS*)-3,5-dihydroxyphenylglycine (DHPG), 3-((2-methyl-1,3-thiazol-4-yl)ethynyl)pyridine (MTEP), 7-(hydroxyimino)cyclopropa[b]chromen-1a-carboxylate ethyl ester (CPCCOEt), and DL-threo-β-benzyloxyaspartic acid (DL-TBOA) were obtained from Tocris Bioscience. D-AP-5, tetrodotoxin (TTX), and ifenprodil were obtained from Ascent. BAPTA tetrapotassium salt, Alexa Fluor 488 and 594, fura-2 AM, and sulforhodamine 101 (SR101) were obtained from Invitrogen.

Electrophysiology. The recording chamber and manipulators were mounted on a moveable top plate platform (MP MTP-01; Scientifica). Patch-clamp recordings were made using pipettes (2–4 MΩ) containing an internal solution of the following composition (in mM): 120 KMeSO$_4$, 10 HEPES, 0.1 EGTA, 4 Na$_2$ATP, and 0.5 GTP, adjusted to pH 7.3–7.4 with KOH (osmolarity 285–290 mOsm). Currents were recorded using a Multiclamp700B amplifier, digitized with a Digidata 1440A, and acquired and analyzed using pClamp (Molecular Devices). Voltage-clamp recordings were made at −60 mV, and, for current-clamp recordings, neurons were held at ~5 mV negative to firing threshold. Cells with ≥20% change in access resistance were excluded. SICs were analyzed using the Event Detection protocols in the Clampfit routine of pClamp. Events were accepted as SICs if their amplitude was >20 pA and their time-to-peak (indicated as rise time in figures) was >20 ms. Data were exported to SigmaPlot (Jandel) for additional analysis and plotting.

Inhibition of [Ca^{2+}]$_i$ signaling. In experiments in which astrocytic calcium signaling was selectively inhibited, we used high BAPTA (40 mM) infusion (Serrano et al., 2006; Gómez-Gonzalo et al., 2010). Astrocytes were patch clamped with pipettes containing internal solution of the following composition (in mM): 30 Cs-methanesulphonate, 10 HEPES, 4 Na$_2$ATP, 5 KCl, 0.5 GTP, 1 MgCl$_2$, and 40 BAPTA, pH 7.4 (osmolarity 290 mOsm). Alexa Fluor 488 (0.1 mM) was included in this solution to enable visualization of filled cells. In corresponding control experiments, the internal solution omitted BAPTA and was of the following composition (in mM): 120 Cs-methanesulphonate, 10 HEPES, 4 Na$_2$ATP, 5 KCl, 0.5 GTP, 1 MgCl$_2$, 5 EGTA, and 0.1 Alexa Fluor 488, pH 7.4 (osmolarity 280 mOsm). Cells were identified by their morphology and electrophysiological properties (Parri et al., 2010). Astrocytes were held at −80 mV for 30 min to allow filling, and a TC neuron was then patched within the filled astrocytic field to record SICs. The neuronal recording solution was standard KMeSO$_4$ internal (above) with 0.1 mM Alexa Fluor 594 for visualization. To avoid dye/BAPTA leakage, electrode tips were filled with control internal excluding BAPTA and/or dye during cell approach and seal formation. For these experiments, slices were treated with 100 μM DHPG in the storage solution in the presence of kynurenic acid (2 mM) to induce LTE before recording.

Synaptic stimulation. Synaptic stimulation was achieved with a computer-controlled constant-current isolated stimulator (STG1002; Multichannel Systems) and bipolar electrodes that were placed typically >200 μm from the recorded neurons. Somatosensory stimulation was

achieved by placing a bipolar electrode on the medial lemniscus (lemniscal), and CT afferents were stimulated by a bipolar electrode on the internal capsule. To investigate the effects of continual afferent synaptic input, we devised a protocol, written in the STG1002 interface software, that allowed synaptic stimulation over time without causing synaptic transmission rundown in the isolated VB thalamus *ex vivo* preparation. This was achieved using an intermittent repetitive train stimulation (RTS) (10–20 × 2 ms, 100–800 μA stimulations at 50 Hz every 5–10 s) comparable with the ~50 Hz bursts that occur *in vivo* during whisking and CT activity (Deschênes et al., 2003; Steriade, 2006). At the selected stimulus intensity, elicited postsynaptic currents (PSCs) were 50–60% of maximal and did not result in synaptic depletion during continual stimulation for up to 30 min (see Fig. 2B,C). In experiments comparing spontaneous astrocytically derived SICs with synaptic-transmission-generated PSCs, PSCs were evoked by a train of 10 × 2 ms stimuli delivered at 50 Hz to lemniscal or corticothalamic inputs.

Fluorescence imaging. In these experiments, slices were loaded with fura-2 AM (Invitrogen) after a post-cutting recovery period of 1 h. This was done by incubating for ~50 min at 30°C with 5 μM of the indicator dye and 0.01% pluronic acid. Under these conditions, astrocytes are preferentially loaded (Parri et al., 2001). For astrocytic identification, slices were also loaded with 1 μM sulforhodamine 101, according to the *in vitro* methods of Kafitz et al. (2008). The recording chamber and manipulators were mounted on a motorized moveable bridge (Luigs and Neumann), and fluorescence dyes were excited using an Optoscan monochromator system, fitted to a Nikon FN1 upright microscope; filter cubes for selective fura-2 and SR101 imaging were obtained from Chroma Technology Corp. Images of slice areas of 444 × 341 μm were routinely acquired every 5 s with a 20× objective lens (numerical aperture 0.8) using an ORCA ER CCD camera (Hamamatsu) and analyzed using Simple PCI software (Hamamatsu). Only cells positive for the astrocytic marker SR101 were included in the analyses.

Ratiometric calcium values over time for specific regions of interest were exported and analyzed using custom-made software written in the Matlab (MathWorks) mathematics programming environment. Data were initially de-noised using automated one-dimensional wavelet decomposition and normalized to individual minima without rescaling. The number of active cells in each slice was determined using an automated search of the data to identify voxels in which the amplitude exceeded 2 SDs of the mean. The number of events in each condition was established using an automated search for local maxima in which peaks were identified as samples with an amplitude that is 2 SDs or greater than its neighbors. The mean amplitude was then calculated using the mean of these local maxima for all cells in each condition. The area under the curve (AUC) for each cell was computed based on the absolute power of all events as a function of the number of suprathreshold maxima in that condition.

Statistics. All quantitative data in the text and figures are presented as mean ± SEM unless otherwise stated. Significance was calculated using multivariate ANOVA and unpaired or paired Student's *t* test as appropriate. Kolmogorov–Smirnov tests were used for population distribution comparisons. Linear correlations (r^2) were tested using Pearson's rank correlation. Statistical significance in the figures is indicated as $^*p < 0.05$, $^{**}p < 0.01$, or $^{***}p < 0.005$.

Results

VB slices exhibit spontaneous slow inward currents

We have previously described SICs in TC neurons in the rat VB (Parri et al., 2001). The currents emerged spontaneously and were correlated with neighboring astrocytic [Ca^{2+}]$_i$ elevations. SICs were blocked by NMDA-R antagonists, and SICs could also be evoked by depolarization of neighboring patch-clamped astrocytes (Parri et al., 2010). Here, spontaneous SICs were observed in the presence of TTX at low frequencies (0.07 ± 0.01 SICs/min; *n* = 39 neurons), of the order of ~0.001 Hz (Fig. 1A,B). The mean amplitude of the SICs was 124.7 ± 0.5 pA (ranging from 24.5 to 685.9 pA), and the mean rise time was 128.4 ± 0.5 ms (ranging from
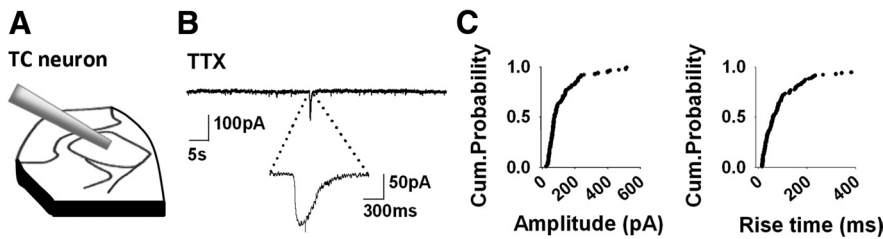
Figure 1. Spontaneous slow inward currents in VB thalamus TC neurons. *A*, Schematic drawing of the VB thalamus slice preparation showing the position of the TC neuron recording electrode in the VB nucleus. *B*, Current recording in the presence of TTX (1 μM) showing an example of a spontaneous SIC. *C*, Cumulative probability graphs showing the distribution of SIC amplitude and rise time ($n = 122$ SICs from 39 TC neurons).
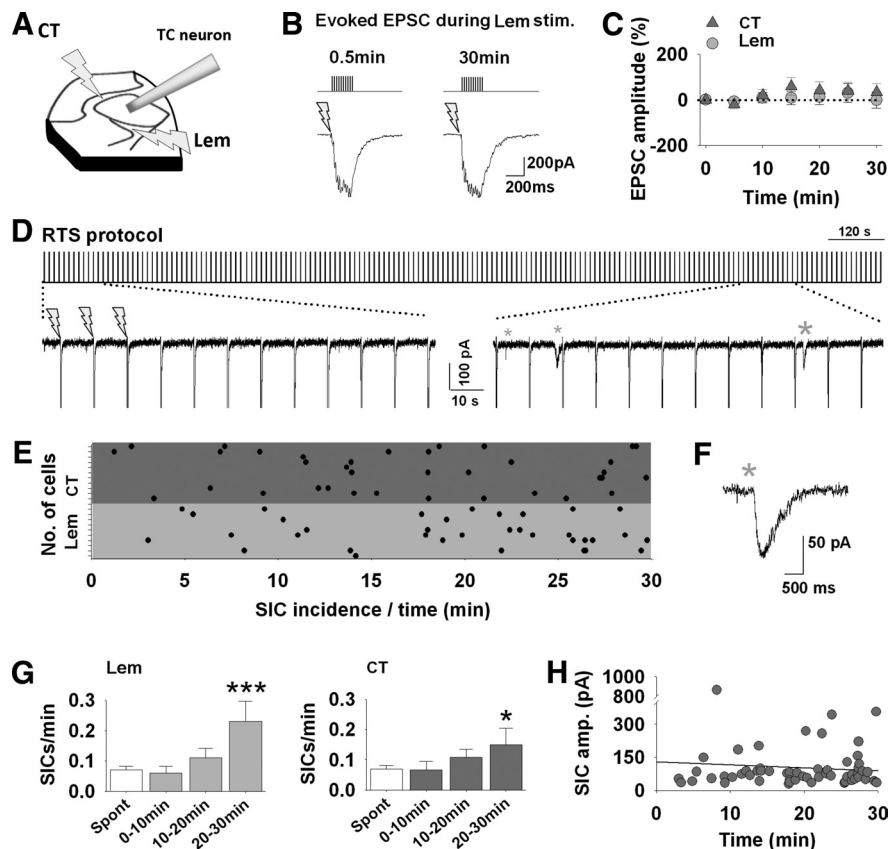
Figure 2. Afferent activity induces a time-dependent increase in SIC emergence. *A*, Schematic drawing of the VB thalamus slice preparation, illustrating the position of the TC neuron recording patch electrode and stimulating electrodes (lightning bolts) on lemniscal (Lem) and CT afferents. *B*, Example traces show evoked EPSCs in response to lemniscal stimulation elicited by stimulus trains (gray patterns above) at times indicated during an RTS protocol, in which trains were elicited every 10 s. *C*, Mean change in evoked EPSC amplitude over a 30 min RTS protocol (10–20 × 2 ms pulses of 100–800 μA at 50 Hz every 5–10 s) for lemniscal ($n = 9$) and CT ($n = 12$) inputs, showing constancy of responses. *D*, Current recording from a TC neuron during RTS (top trace) applied to lemniscal input. Each upward deflection is a 10 × 2 ms, 50 Hz stimulus "train." Bottom traces show enlarged sections from the beginning and end of the experiment, with lightning bolts indicating EPSCs evoked by the stimulus trains. Emergent astrocyte-derived SICs are indicated by asterisks. *E*, Raster plot displaying SIC incidence (black dots) during an RTS protocol for CT ($n = 12$; dark gray) and lemniscal ($n = 10$; light gray) inputs. Each row represents a different TC neuron recording. *F*, Enlarged SIC from *D* indicated with larger asterisk. *G*, Mean spontaneous SIC frequency compared with frequency during RTS for lemniscal and CT stimulation. *H*, Scatter plot and line of best fit showing a lack of correlation between SIC amplitude and time over the 30 min stimulation protocol.

20.3 to 1597.4 ms) (Fig. 1*C*), consistent with our previous observations of these currents (Parri et al., 2001).

Afferent activity increases SIC frequency over time

In vivo, the thalamus constantly receives afferent lemniscal input during whisking or consciousness state-dependent CT input (Deschênes et al., 2003; Steriade, 2006). Therefore, to investigate

the effect of afferent activity on astrocyte–neuron signaling, we used a continual stimulus protocol consisting of brief intermittent trains (RTS; see Materials and Methods), composed of bursts at 50 Hz. Recordings were made from VB thalamus TC neurons during application of RTS onto lemniscal or CT afferent pathways (Fig. 2*A*,*B*). When applied over a 30 min period, the amplitude of the stimulus-evoked EPSCs was not affected significantly during either lemniscal ($n = 9$ neurons; paired t test, $p \geq 0.48$) or CT ($n = 12$; $p \geq 0.15$) afferent stimulation (Fig. 2*C*).

However, analyzing the emergence of SICs during the 30 min period of stimulation (Fig. 2*D–F*) revealed that the mean SIC frequency (Fig. 2*G*) in the interval 20–30 min was significantly higher when compared with spontaneous SIC frequency (0.07 ± 0.01 SICs/min) for both lemniscal (0.23 ± 0.07 SICs/min; $n = 10$ neurons; t test, $p < 0.001$) and CT (0.15 ± 0.05; $n = 12$ neurons; $p < 0.05$) stimulation. SIC amplitude, however, was not increased (Pearson's correlation, $r^2 = 0.008$; $p = 0.5$) over the course of stimulation (Fig. 2*H*).

Afferent activity induces a long-term enhancement of glial signaling

Previous studies in other brain areas have shown that SICs are generated after acute trains of synaptic stimuli (Fellin et al., 2004; D'Ascenzo et al., 2007), consistent with stimulus-evoked astrocytic calcium elevations triggering vesicular GT release (Araque et al., 2000; Bezzi et al., 2004). However, our data suggested that either the astrocytic glutamate release frequency was being modified by the repetitive stimuli or the astrocytes were becoming more sensitive to the afferent stimulation, which was then evoking glutamate release.

To investigate this, we made recordings from TC neurons after cessation of RTS input to both afferent pathways. We found that SICs at increased frequency continued for >1 h in the absence of afferent stimulation (Fig. 3*A*,*B*), indicating a change in astrocytic glutamate release, which is independent of continuing afferent activity (ANOVA $p < 0.001$) (Fig. 3*B*). This phenomenon was termed LTE of astrocyte–neuron signaling. The increase in SIC frequency after termination of RTS (control, 0.086 ± 0.01 SICs/min, $n = 77$ neurons; LTE, 0.33 ± 0.06 SICs/min, $n = 61$; t test, $p < 0.001$) (Fig. 3*C*) was not affected by the presence of TTX (1 μM) ($115 \pm 21.9\%$ of control; $n = 13$; paired t test, $p = 0.5$) (Fig. 3*D*). Furthermore, SIC kinetic parameters were unaffected (amplitude: control, 159.9 ± 9.4 pA; LTE, 143.7 ± 6.6 pA; Student's t test, $p = 0.16$; rise time: control, 117.2 ± 20.8 ms; LTE, 133.0 ± 13.9 ms; $p = 0.5$; decay time:

control, 831.4 ± 336.8; LTE, 505.2 ± 62.4 ms; p = 0.2; Q: control, 185.8121 ± 133.2727 mC; LTE, 52.0394 ± 5.6785; p = 0.2), supporting the notion that LTE of SICs is the result of a plasticity of astrocytic GT release rather than a postsynaptic neuron modification (Redman, 1990).

## LTE at different developmental stages
The somatosensory thalamus undergoes postnatal developmental changes, including receptor expression (Golshani et al., 1998) and synaptic connectivity (Matthews et al., 1977; Ivy and Killackey, 1982). These changes are complete by P21. We therefore investigated whether LTE and its induction exhibited a developmental profile by inducing LTE in VB thalamus slices from rats at varying ages over the first 3 postnatal weeks. There was no significant difference in spontaneous SIC frequency across this period of maturation (Fig. 4A, B). However, the degree of LTE that could be induced changed during maturation (Fig. 4A, B). In the first postnatal week (P6–P7), SIC frequency was increased on average by 123.4% after RTS (control, 0.11 ± 0.03 SICs/min, n = 43 neurons; post-RTS, 0.26 ± 0.06 SICs/min, n = 13; t test, p = 0.018) (Fig. 4B). In the second week (P10–P14), the increase was 265.2% (control, 0.07 ± 0.01 SICs/min, n = 44; post-RTS, 0.24 ± 0.08 SICs/min, n = 11; p = 0.0002), and, at the end of the third week (P20–P23), LTE was 696.4% (control, 0.12 ± 0.04, n = 42; post-RTS, 0.95 ± 0.41, n = 21; p = 0.006) (Fig. 4B).

To test whether the increase in LTE induction could be explained by a maturation-dependent increase in glutamate release by our RTS protocol, we recorded the sum of the postsynaptic charge (EPSC Q) evoked by lemniscal and CT stimulation, to provide a measure of the excitatory input onto each neuron. EPSC Q remained constant throughout maturation (week 1, 0.37 ± 0.12 mC; week 2, 0.43 ± 0.13 mC; week 3, 0.49 ± 0.08 mC) and did not significantly differ between any groups during the developmental stages (t test, p ≥ 0.36) (Fig. 4C). In addition, LTE SIC frequency was not correlated to EPSC Q for individual cells (Pearson's correlation, r^2 = 0.02; p = 0.4) (Fig. 4D). These data indicate that the increase in SIC frequency is not simply a function of the amount of glutamatergic input into the VB thalamus and that the relative synaptic glutamate signaling that a neuron receives is not correlated with the amount of nonsynaptic astrocytic glutamate input.

RTS induces an mGluR-dependent increase in astrocytic excitability
Astrocytic excitability is defined by elevations in intracellular calcium levels. Indeed, VB thalamus astrocytes display spontaneous Ca^{2+} oscillations (Parri and Crunelli, 2001, 2003; Parri et al., 2001). Spontaneous and agonist-evoked astrocytic elevations are correlated to SICs (Parri et al., 2001). It might therefore be expected that the increased SIC signaling seen in LTE would be associated with an increased astrocytic excitability manifested as changes in $[Ca^{2+}]_i$ elevations (Pasti et al., 1997).

We imaged VB thalamus slices loaded with the ratiometric Ca^{2+}-sensitive dye fura-2 and the astrocyte-selective dye SR101
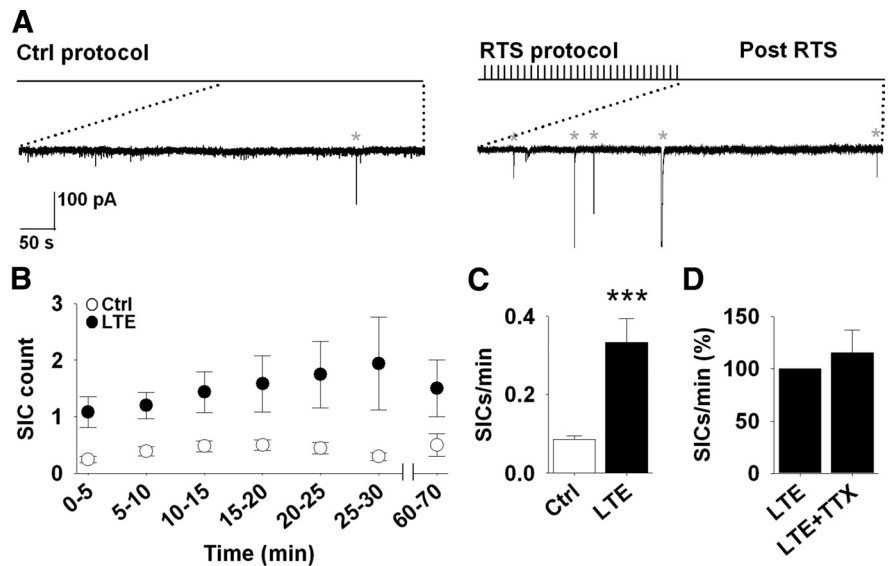
Figure 3. Afferent activity induces a long-term enhancement of glial signaling. **A**, SICs in control (left) and after cessation of 60 min simultaneous lemniscal and CT RTS (right). SICs are marked with asterisks. **B**, Mean SIC incidence in 5 min bins after RTS cessation (black circles; n = 61) compared with nonstimulated controls (white circles; n = 77; ANOVA, p < 0.001). **C**, Pooled data from **B** illustrating overall SIC frequency increase. **D**, Mean percentage change in SIC frequency illustrating the lack of effect of TTX on LTE SIC incidence (n = 13). Ctrl, Control.

before and after RTS (Fig. 5A, B.). This approach revealed significant increases in the number of active astrocytes (254.4 ± 21.2%; n = 5 slices; t test, p < 0.005), the frequency of $[Ca^{2+}]_i$ elevations per astrocyte (171.1 ± 11.6%; n = 145 astrocytes; p < 0.005), and the AUC of individual $[Ca^{2+}]_i$ elevations (202.4 ± 16.7%; n = 145 astrocytes; p < 0.005) after RTS (Fig. 5C--E). However, the amplitude of $[Ca^{2+}]_i$ elevations was unaffected (101 ± 10.4%; n = 145 astrocytes; p = 54) (Fig. 5F).

The observed changes after RTS were prevented in the presence of the group I mGluR1 and mGluR5 antagonists CPCCOEt (100 μM) and MTEP (50 μM) during the stimulation period (Fig. 5C–F). The number of active astrocytes was 99.0 ± 12.1% of control (n = 3 slices; p = 0.14), the frequency of $[Ca^{2+}]_i$ elevations per astrocyte was 100.22 ± 9.42% of control (n = 41 astrocytes; p = 0.32), the AUC of $[Ca^{2+}]_i$ elevations was 114.5 ± 38.4% of control (n = 41 astrocytes; p = 0.08), and the amplitude of the $[Ca^{2+}]_i$ elevations was 98.08 ± 8.2% of control (n = 41; p = 0.45).

LTE of SICs requires mGluR activation
To investigate the pharmacology of the induction of LTE of SICs, we applied the RTS protocol to lemniscal and CT afferents in the presence or absence of MTEP (50 μM) and CPCCOEt (100 μM). SICs were then recorded after stimulus cessation and wash off of antagonists (Fig. 6A). Whereas SIC frequency was increased (0.25 ± 0.06; n = 29) significantly by RTS compared with control unstimulated slices (0.069 ± 0.01 SICs/min; n = 53 neurons; t test, p < 0.005) in the absence of mGluR antagonists; this increase was prevented in the presence of the mGluR antagonists MTEP and CPCCOEt during the stimulus induction phase (0.056 ± 0.02; n = 8; p = 0.6). However, the induction of LTE was not significantly affected when MTEP (0.17 ± 0.05 SICs/min; n = 15; p = 0.07) or CPCCOEt (0.19 ± 0.05 SICs/min; n = 10; p < 0.005) was applied alone, indicating that synaptically released glutamate induces LTE via group I mGluR-mediated pathways.

To confirm a role for group I mGluRs, we mimicked synaptic mGluR activation by exposure (≥60 min) to the selective group I
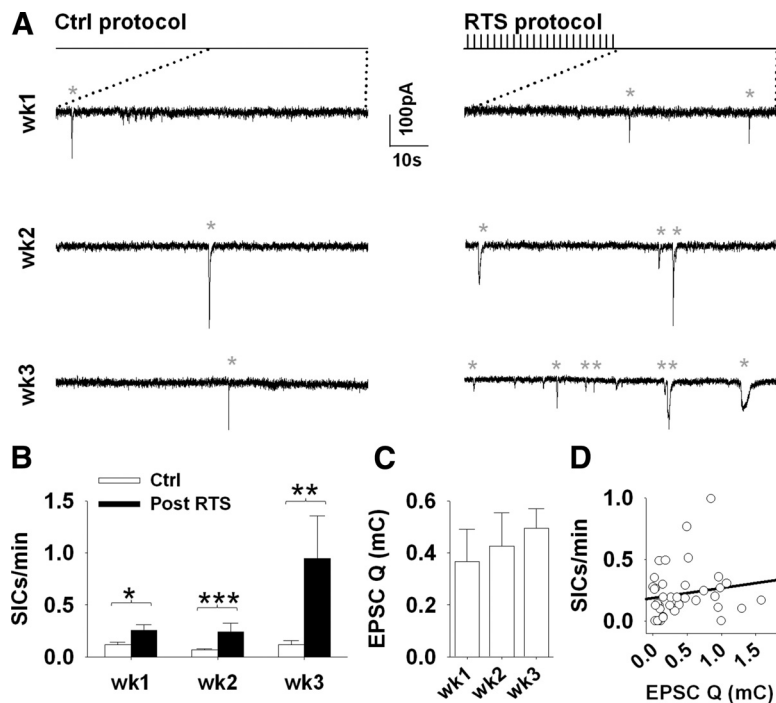
Figure 4. LTE at different developmental stages. **A**, Traces illustrate SICs in control conditions (left) and after cessation of 60 min of simultaneous lemniscal and CT RTS (right), during week 1 (top), week 2 (middle), and week 3 (bottom). **B**, Bar graph showing the mean SIC frequency in control conditions compared with post-RTS conditions for each postnatal week (week 1, $n = 43$ vs 13; week 2, $n = 44$ vs 11; week 3, $n = 42$ vs 21). **C**, Bar graph showing the mean summated lemniscal and CT EPSC charge for each age group tested before SIC recordings. **D**, Scatter plot and line of best fit showing a lack of correlation between SIC frequency and EPSC charge. Ctrl, Control.

mGluR1/mGluR5 agonist DHPG (100 μM) or the mGluR5-selective agonist CHPG (500–1000 μM) and recorded SICs after agonist wash off (Fig. 6B). This revealed that, compared with control (0.069 $\pm$ 0.01 SICs/min; $n = 53$), both mGluR1/mGluR5 activation using DHPG (0.18 $\pm$ 0.07; $n = 24$; t test, $p < 0.05$) and mGluR5-selective activation using CHPG (0.22 $\pm$ 0.09; $n = 20$; $p < 0.05$) resulted in significant LTE. DHPG (100 μM) in conjunction with MTEP (50 μM) also displayed a significant increase in SIC frequency (0.26 $\pm$ 0.07; $n = 6$; $p < 0.001$), indicating that mGluR1 activation is also sufficient to induce LTE.

To determine possible ionotropic glutamate receptor (iGluR) contributions, we applied the RTS protocol in the presence of the broad-spectrum ionotropic glutamate antagonist kynurenic acid (1 mM) and recorded SICs after wash off (Fig. 6C). This demonstrated that SIC frequency was increased after RTS in the presence of kynurenic acid (0.31 $\pm$ 0.06 SICs/min; $n = 38$ neurons; t test, $p < 0.005$) compared with control unstimulated slices (0.087 $\pm$ 0.01 SICs/min; $n = 76$) and was not different from LTE elicited in the absence of kynurenic acid (0.26 $\pm$ 0.08 SICs/min; $n = 21$; $p = 0.66$). This shows that LTE induction is independent of iGluRs, including NMDA-R activation, which is involved in classical forms of neuronal synaptic long-term potentiation (Malenka and Nicoll, 1993; Daw et al., 2007).

Another possible contributory mechanism to LTE was that repetitive synaptic afferent activity, and the resultant glutamate release, increased excitatory amino acid transporter-mediated astrocytic glutamate uptake, consequently elevating glutamate content and acting to increase the frequency of glutamate release events. To test this hypothesis, we applied the RTS protocol in the presence of the GLT-1 and GLAST excitatory amino acid transporter inhibitor DL-TBOA (100–150 μM) and again recorded

SICs from TC neurons after stimulus cessation and inhibitor washout. The results (Fig. 6D) show that SIC frequency was increased after RTS in the presence of TBOA (0.47 $\pm$ 0.12 SICs/min; $n = 10$ neurons; $p < 0.05$) compared with control unstimulated slices (0.19 $\pm$ 0.03 SICs/min; $n = 11$). The magnitude of LTE induced in the absence of TBOA (0.51 $\pm$ 0.15 SICs/min; $n = 11$) was not significantly different from LTE induced in its presence ($p = 0.86$). Increased glutamate uptake therefore does not play a role in synaptically induced LTE.

Together, these data confirm that either mGluR5 or mGluR1 activation is sufficient for LTE induction.

## Astrocytic glutamate release is $[Ca^{2+}]_i$ dependent

Calcium imaging experiments (Fig. 5) indicated increased astrocytic oscillation frequency in LTE associated with increased SIC frequency. To determine whether the SICs were $[Ca^{2+}]_i$ dependent, we loaded astrocytes locally via patch pipette with the calcium chelator BAPTA. LTE was first induced by incubating slices with 100 μM DHPG (>1 h), and the slice was then transferred to the recording chamber. An astrocyte was patched with a high-BAPTA-containing solution and Alexa Fluor 488 to enable visualization of the extent of astrocyte syncytium filling (Fig. 7A). After a loading period of 30 min, a neuron within the filled astrocyte field was patched and SICs were recorded. In control experiments, to counteract possible effects of dilution of intracellular contents, an identical protocol was followed except that the internal astrocyte patch solution did not contain high BAPTA. SIC frequency was significantly reduced when astrocytic patch pipette contained BAPTA (LTE, 1.26 $\pm$ 0.35 SICs/min, $n = 8$ slices; BAPTA, 0.39 $\pm$ 0.11, $n = 7$; t test, $p < 0.05$) (Fig. 7B,C), indicating that astrocytic glutamate release events underlying SICs are indeed $[Ca^{2+}]_i$ dependent.

Glial signaling in the VB thalamus targets extrasynaptic NMDA receptors

NMDA receptors vary in subunit composition and can be differentially expressed on neurons (Cull-Candy et al., 2001). Indeed, in developing VB thalamus, it is known that there is a switch in the composition of synaptic NMDA-Rs from NR2B-containing to NR2A-subunit-containing receptors in the first 2 postnatal weeks (Liu et al., 2004b; Arsenault and Zhang 2006).

We used this situation to probe the functional neuronal targets of LTE SICs by comparing the pharmacological sensitivity of evoked synaptic currents and SICs after LTE induction (Fig. 8A). LTE SICs were confirmed to be NMDA-R mediated (Fig. 8B) because the charge transfer (Q) of SICs after LTE was found to be significantly reduced after 50 μM D-AP-5 (Q, 9.3 $\pm$ 6.5% of control; $n = 6$ neurons; paired t test, $p < 0.005$). Furthermore, LTE SICs were found to be substantially mediated by an NR2B-subunit-containing component because ifenprodil (10 μM) significantly reduced the LTE SIC charge transfer (Q, 44.3 $\pm$ 20.8% of control; $n = 6$; $p < 0.05$) (Fig. 8C). Spontaneous control SICs
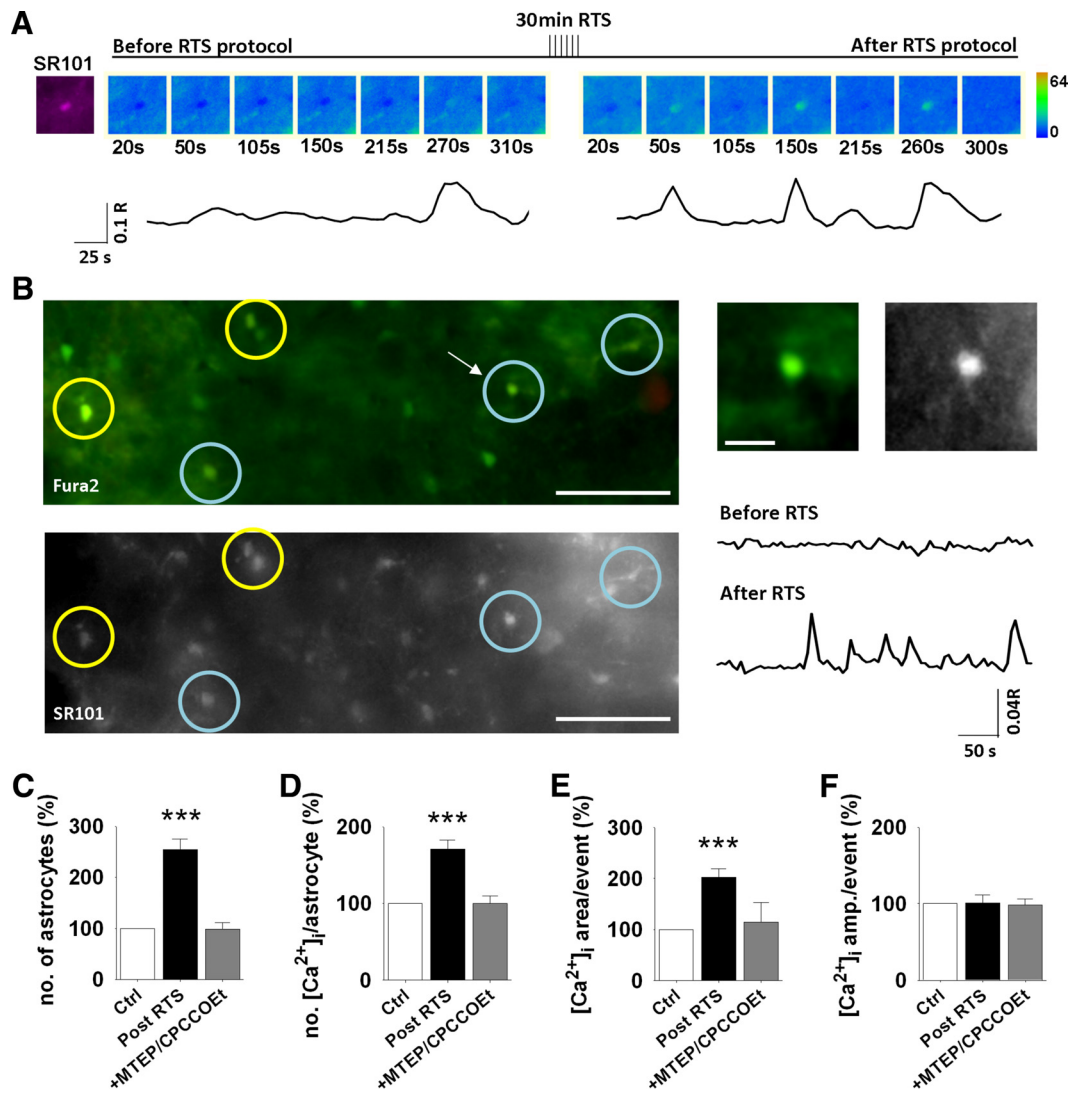
Figure 5. RTS induces mGluR-dependent increase in astrocytic excitability. **A**, Calcium elevations in a single astrocyte before and after RTS protocol in a slice loaded with SR101 and fura-2. Leftmost display is image acquired with 540 nm excitation to reveal SR101. To the right are pseudocolor images of 340/380 nm excitation ratios at indicated acquisition times during the experiment. Trace below displays corresponding plot of ratio values before (left) and after (right) 30 min RTS protocol. **B**, Green fluorescence image (380 nm) of a VB thalamus slice loaded with fura-2 showing the position, spatial distribution, and number of active astrocytes before and after RTS protocol. Position of astrocytes spontaneously active both before and after RTS are circled yellow, and those active only after RTS are circled blue. Scale bar, 50 μm. Panel below shows SR101 fluorescence of the same field to illustrate colocalization of SR101 staining with active cells. Enlarged image of the astrocyte indicated with an arrow is shown on the top right. Scale bar, 10 μm. Traces on the bottom right are from the same astrocyte showing the lack of $[Ca^{2+}]_i$ elevations before the RTS (top) and the emergence of Ca signaling after RTS (bottom). **C–F**, Summary of astrocytic $[Ca^{2+}]_i$ signaling parameters in control and after RTS (post-RTS, $n = 5$ slices; MTEP/CPCCOEt, $n = 3$ slices). Ctrl, Control.

displayed a similar pharmacological profile, being inhibited significantly by both D-AP-5 (Q, 4.6 ± 4.6% of control; $n = 5$; $p <$ 0.005) and ifenprodil (Q, 11.02 ± 8.3% of control; $n = 3$; $p <$ 0.01). In contrast, neuronal postsynaptic currents were insensitive to ifenprodil for both lemniscal (amplitude, 101.3 ± 7.8% of control; $n = 7$ neurons; $p = 0.9$) and CT (amplitude, 106.5 ± 25.5% of control; $n = 6$; $p = 0.8$), whereas D-AP-5 proved to inhibit both lemniscal (amplitude, 31.0 ± 7.4% of control; $n = 7$; $p < 0.005$) and CT (amplitude, 23.3 ± 9.1%; $n = 7$; $p < 0.005$) (Fig. 8D). Therefore, synaptically and astrocytically released glutamate does not target the same population of NMDA receptors, and, by definition, SICs activate extrasynaptic receptors.

**Astrocytic LTE increases spontaneous TC neuron excitation**

We next investigated how the LTE of astrocytic glutamate release affected the activity of TC neurons under physiological conditions.

Recordings were conducted close to tonic firing mode corresponding to the awake condition (Sherman, 2001). After LTE, induced by lemniscal RTS stimulation, the frequency of transient, slow depolarizing potentials (SDPs) (control, 0.056 ± 0.03 events/min; $n = 7$) increased significantly (RTS, 0.77 ± 0.36; $n = 5$; t test, $p < 0.05$) (Fig. 9A,B). These, when sufficiently large, were able to elicit bursts of action potentials (APs) that we termed slow depolarization bursts (SDBs). Importantly, SDPs persisted in the presence of TTX and displayed similar properties to SICs (SDP amplitudes: LTE, 5.0 ± 0.28 mV, $n = 117$ SDPs from 5 neurons; TTX, 4.67 ± 0.99 mV, $n = 16$ SDPs from 2 neurons; Student's t test, $p = 0.7$; time-to-peak: LTE, 98.45 ± 8.28 ms; TTX, 136.37 ± 30.0 ms; Student's t test, $p = 0.13$; total duration: LTE, 297.15 ± 22.15 ms; TTX, 392.71 ± 59.71; Student's t test, $p = 0.14$).

The nonsynaptic release of astrocytic glutamate would be predicted to be able to excite localized groups of neurons in the VB
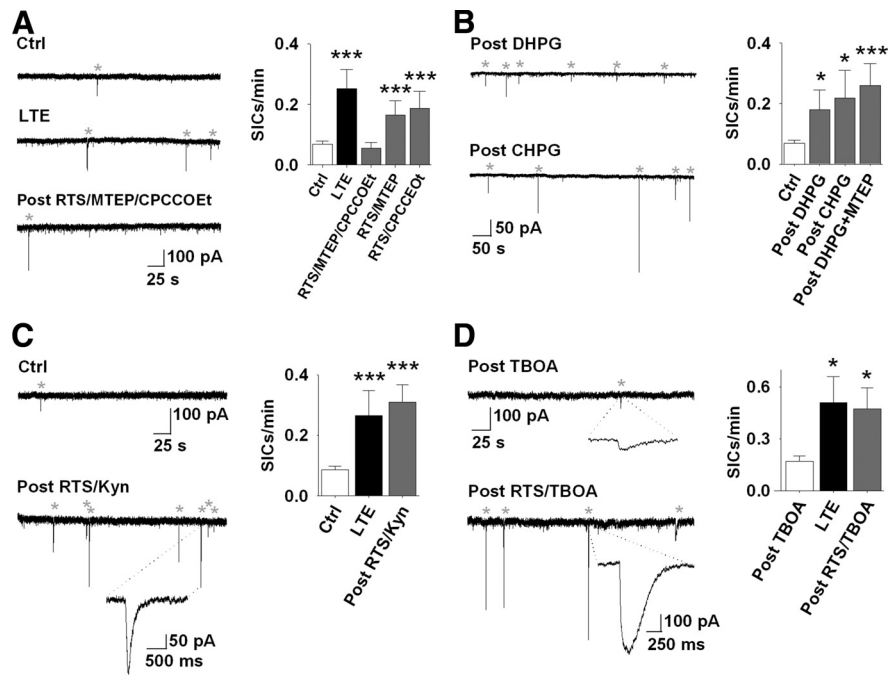
Figure 6. LTE of SICs requires mGluR activation. **A**, Traces on the left illustrate SIC recordings in control conditions without synaptic stimulation (top), after RTS protocol induced LTE (middle), and after RTS protocol conducted in the presence of group I mGluR antagonists (bottom). SICs are indicated with asterisks. Bar graph to the right summarizes results indicating significance of LTE induced in the different conditions (control, $n = 53$ neurons; LTE, $n = 29$; RTS/MTEP (50 μM) plus CPCCOEt (100 μM), $n = 8$; MTEP, $n = 15$; CPCCOEt, $n = 10$). **B**, Traces show SIC recordings after exposure to group I mGluR agonists. Bar graph summarizes results illustrating LTE induction by mGluR1/5 (DHPG at 100 μM; $n = 24$) and mGluR5 (CHPG at 500–1000 μM; $n = 20$) agonists as well as mGluR1 activation by DHPG in the presence of MTEP ($n = 6$). **C**, Trace from control experiment and after RTS in the presence of kynurenic acid (Kyn; 1 mM). Bar graph summarizes results illustrating LTE induced by the RTS protocol with and without kynurenic (control, $n = 76$ neurons; LTE, $n = 21$; post-RTS/kynurenic, $n = 38$). **D**, Top trace from control experiment in which the slices have been exposed to TBOA (100–150 μM) in absence of synaptic stimulation and SICs recorded after TBOA washout. Trace below shows SICs after RTS in the presence of TBOA. Bar graph on the right summarizes SIC frequency in different experiments (post-TBOA, $n = 11$ neurons; LTE, $n = 11$; post-RTS/TBOA, $n = 10$). Ctrl, Control.
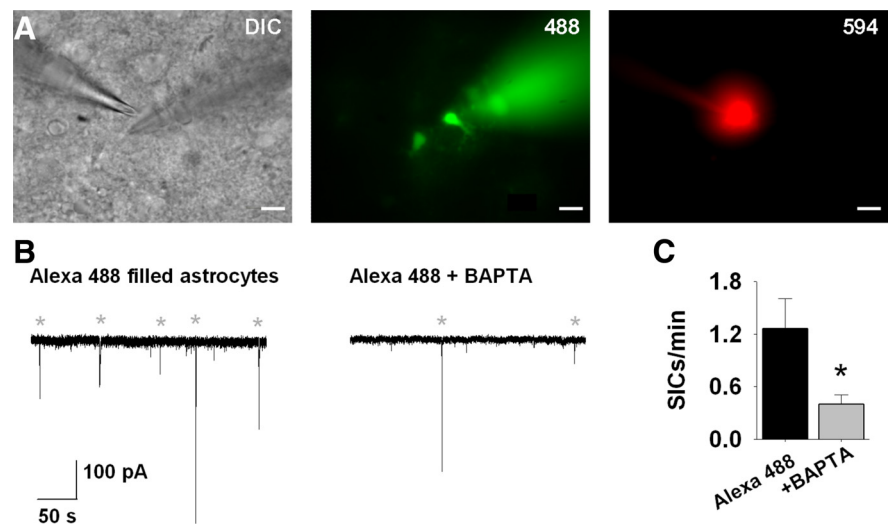
Figure 7. LTE is dependent on astrocytic $[Ca^{2+}]_i$. **A**, Infrared differential interference contrast image on the left illustrating recording arrangement from a neuron (left patch pipette) and astrocyte (right patch pipette). The middle display image acquired with 488 excitation illustrates the spread of Alexa Fluor 488 and BAPTA-containing internal in neighboring astrocytes. Image on the right reveals the Alexa Fluor 594-filled TC neuron. Green and red filling electrodes are visible in respective images. Scale bars, 10 μm. **B**, Left, Recording from a neuron in which local astrocytic syncytium was filled with control Alexa Fluor 488 solution after LTE induction with DHPG pretreatment; right, trace showing a recording in which the local astrocytes were filled with a pipette solution containing 40 mM BAPTA and Alexa Fluor 488 after LTE induction. **C**, Bar graph summarizes results illustrating LTE with or without BAPTA (Alexa Fluor 488, $n = 8$; +BAPTA, $n = 7$).

thalamus (Parri and Crunelli, 2002) as has been found in other brain areas (Angulo et al., 2004; Fellin et al., 2004, 2006a; D'Ascenzo et al., 2007). We therefore used this attribute to establish whether SDPs and SDBs were generated by SICs. Paired recordings were made from neighboring TC neurons (Fig. 9C), which revealed synchronous SICs and coincident SDBs and SICs (Fig. 9D), consistent with SICs eliciting neuronal firing (Fellin et al., 2006b; D'Ascenzo et al., 2007). The amplitudes of SICs in paired recordings were not significantly correlated (Pearson's correlation, $p = 0.8$), nor were SIC amplitude and the number of elicited APs per SDB ($p = 0.7$) (Fig. 9E), indicating a complex and potentially dynamic relationship between astrocytic release and neuronal targets. Analysis of paired recordings also showed that SIC frequency, but not the proportion of synchronized events (control, $3.6 \pm 3.6\%$, $n = 7$ pairs; LTE, $7.6 \pm 4.6\%$, $n = 11$; t test, $p = 0.5$), increased with LTE.

To confirm that the observed depolarizing events were astrocytically mediated, we used the waveforms of SICs recorded in our experiments and injected them into neurons while recording in current-clamp mode (Fig. 9F). Injected SIC current waveforms ($n = 10$ neurons, 96 SDBs) induced similar slow depolarizations and bursts to spontaneously recorded SDP and SDBs ($n = 13$ neurons, 90 SDBs) and generated indistinguishable characteristic firing patterns (interspike intervals, t test, $p \geq 0.3$) (Fig. 9D,F,I). Both the spontaneous and injected SIC-evoked firing patterns were distinct from the stereotypical AP pattern generated during classic low-threshold calcium (I_T) bursts (Jahnsen and Llinás, 1984) ($n = 5$ neurons, 136 I_T bursts) (interspike intervals, t test, $p < 0.05$ between all comparisons) (Fig. 9G-I), illustrating that SDBs are a distinct type of TC neuron firing output.

We further hypothesized that, if SICs underlie SDPs and SDBs, then these events would be inhibited by ifenprodil. Indeed, application of ifenprodil (10 μM) after LTE induction reduced the frequency of SDPs and SDBs to $42.2 \pm 14.1\%$ of the control ($n = 9$ neurons; paired t test, $p < 0.005$) (Fig. 9J,K). Ifenprodil also reduced the number of APs elicited by the remaining SDBs from 4.5 ± 0.5 in control to 2.5 ± 0.2 after ifenprodil, a significant reduction (t test, $p < 0.005$) (Fig. 9L). These results are consistent with ifenprodil-mediated inhibition of neuronal NR2B-containing receptors, thus reducing the amplitude of SICs (Fig. 8C)

and the depolarizations elicited in the neurons.

Consequently, when considered together, these findings suggest that, when the frequency of SIC is increased after LTE, this periodically induces a synchronized excitation of local neurons that persists long after the cessation of the afferent stimulus.
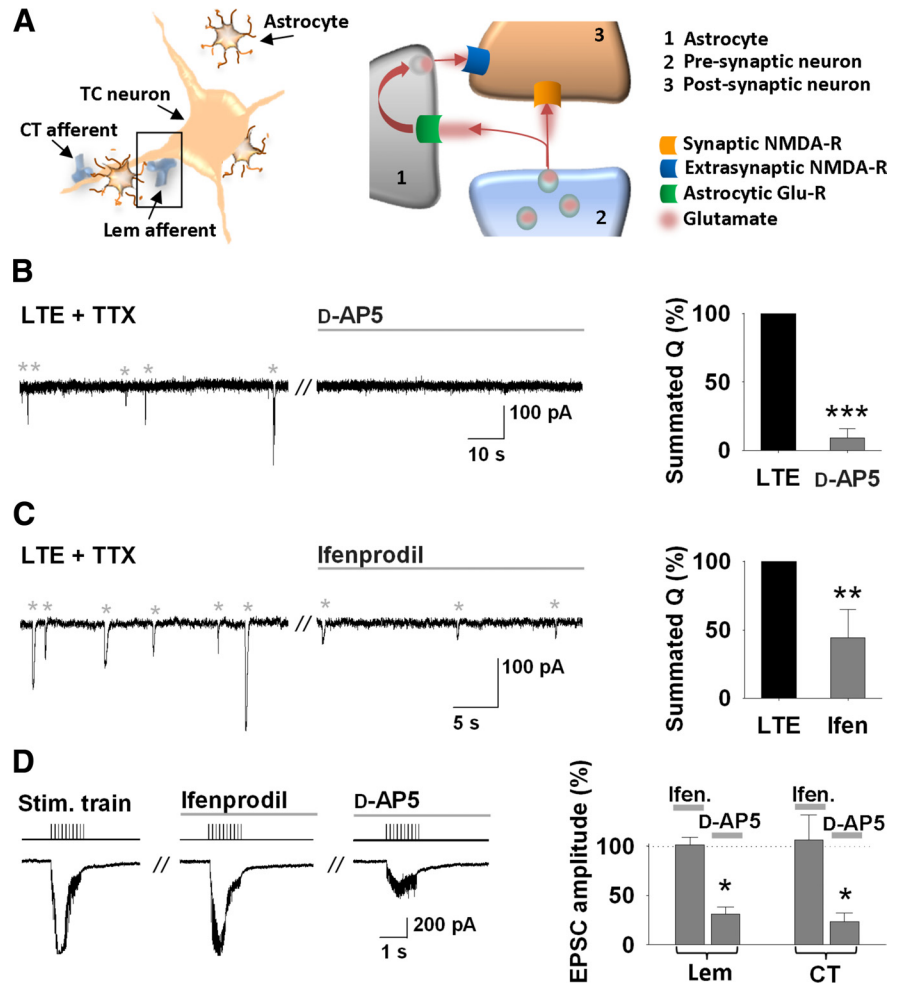
Discussion

Astrocytes and plasticity

In addition to long known roles of astrocytes in homeostatic brain mechanisms, astrocytes also participate in synaptic information transfer in the brain. There is increasing evidence that the release of GTs, such as glutamate, ATP, or D-serine, act at presynaptic and/or postsynaptic targets to modulate synaptic signaling between neurons, which leads to synaptic potentiation (Kang et al., 1998; Yang et al., 2003; Jourdain et al., 2007; Perea and Araque, 2007; Henneberger et al., 2010) or depression (Pascual et al., 2005; Serrano et al., 2006). The model of the tripartite synapse proposes that synaptic neurotransmitter release activates receptors on ensheathing astrocytes, eliciting calcium elevations that lead to gliotransmitter release and resultant synaptic modulation (Araque et al., 1999). Indeed, studies using *in vitro* brain slice preparations of hippocampus and nucleus accumbens have shown that astrocytes can release glutamate, detected as SICs, after acute synaptic stimulation (Fellin et al., 2004; D'Ascenzo et al., 2007). Our findings, however, present an additional scenario, in which afferent input results in long-term signaling changes from astrocytes to neurons. This is therefore a plasticity of astrocytic GT release instigated by afferent activity, in which the subsequently enhanced GT release is not dependent on additional afferent activity.

Figure 8. Glial signaling in the VB thalamus targets extrasynaptic NMDA receptors. *A*, Illustrative diagram of thalamic cellular elements and synaptic afferent arrangement. Boxed area is shown expanded on the right, illustrating the SIC targeting hypothesis to be tested. *B*, Recording of spontaneous LTE SICs in the presence of TTX (1 μM) and summary bar graphs showing their block by D-AP-5 (50 μM) expressed as summated SIC charge (*Q*) transfer (*n* = 6 neurons). *C*, The effect of ifenprodil (Ifen, 10 μM) on LTE SICs (*n* = 6). *D*, EPSC (below) recorded in a TC neuron in response to lemniscal (Lem) stimulation (above) and the effect of NMDA-R antagonists. Bar graphs illustrate normalized data for the afferent inputs during ifenprodil (lemniscal, *n* = 7 neurons; CT, *n* = 6) and D-AP-5 (lemniscal, *n* = 7; CT, *n* = 7) application.

Mechanism of LTE

The somatosensory and corticothalamic afferents stimulated in this study are both glutamatergic, but the induction of LTE was not dependent on the activation of iGluRs as is the case with forms of neuronal plasticity (Malenka and Nicoll, 1993). Although there is no evidence indicating the presence of either AMPA/kainate or NMDA receptors on VB thalamus astrocytes (Parri et al., 2010), NMDA receptors have been shown on cortical astrocytes (Lalo et al., 2006). However, if present in subcortical astrocytes, these receptors are not involved in the form of astrocytic plasticity that we describe here. Instead, we found that the induction of LTE is dependent on the group I mGluR because LTE induction is inhibited by combined antagonism of mGluR5 and mGluR1 and is also induced by exposure to a general group I mGluR agonist and a selective mGluR5 agonist. Although mGluR5 is expressed in neurons and astrocytes in the VB thalamus, an astrocytic locus of action is supported by the preferential expression of mGluR5 RNA in VB thalamus astrocytes (Biber et

al., 1999) and by their major role in mediating synaptically induced [Ca^{2+}]$_i$ elevations (Parri et al., 2010). The identification of this astrocytic modulatory role therefore reveals another function for group I mGluR receptors in the thalamus, in addition to mGluR1a-subtype activation, which underlie the generation of slow sleep oscillations (Hughes et al., 2002; Crunelli and Hughes, 2010) and mGluR1 activation in the thalamic reticular nucleus, which acts to reduce neuronal synchronization by modifying gap-junctional coupling (Landisman and Connors, 2005).

In conjunction with increased SICs in LTE, we observed an increase in astrocytic excitability in the form of increased [Ca^{2+}]$_i$ elevations. There is much present debate on the role of [Ca^{2+}]$_i$ in GT release, whether vesicular or other mechanisms are involved (Hamilton and Attwell, 2010), and indeed whether GT release has physiological impact. Notably, a recent study on astrocytic D-serine release showed that clamping astrocytic [Ca^{2+}]$_i$ changes prevented its release and inhibited Schaffer collateral–CA1 LTP (Henneberger et al., 2010). Another study using transgenic approaches to knock-out astrocytic calcium signaling concluded that astrocytic calcium signaling had little or no role in brain function because its inhibition had no effect on the electrophys-
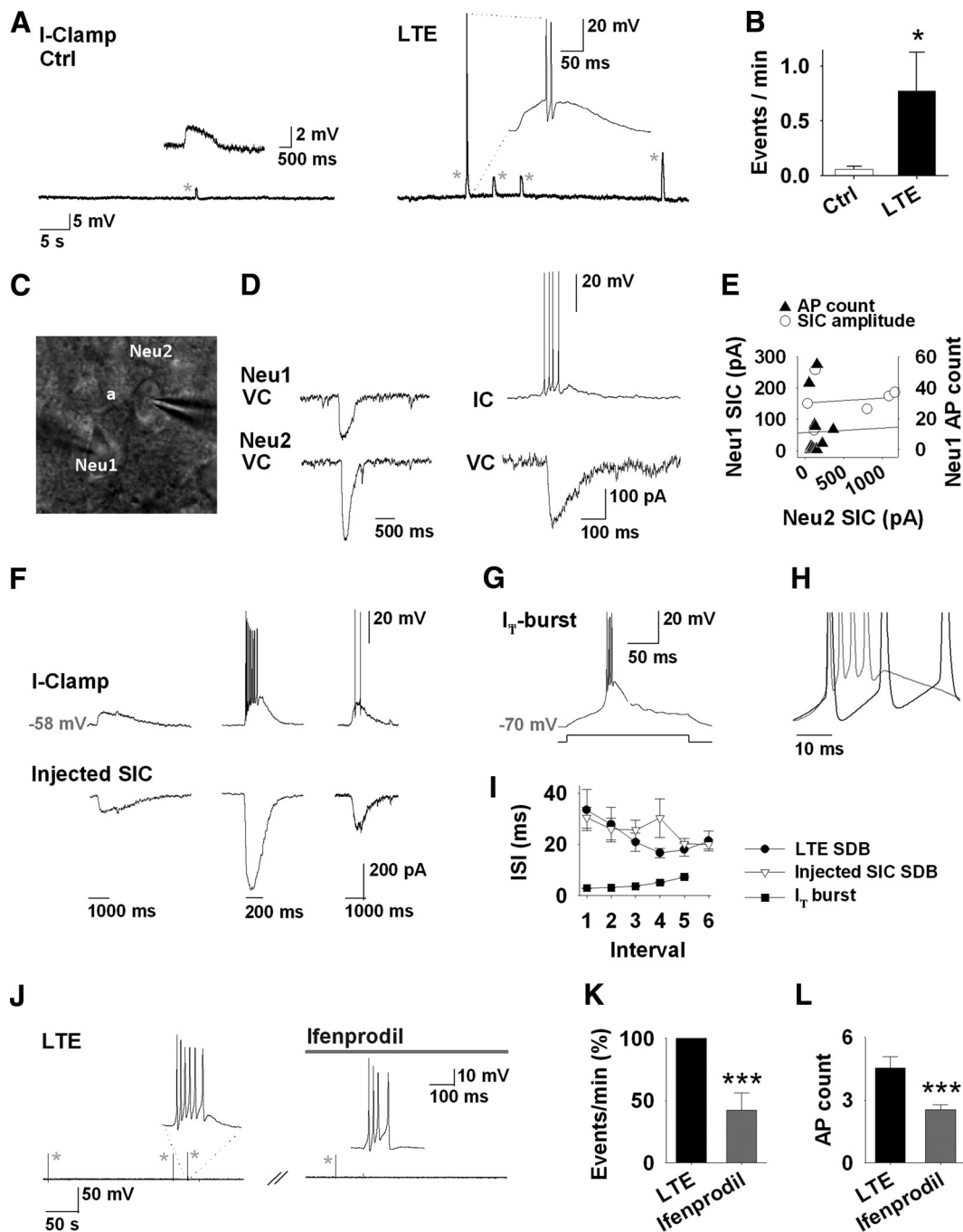
Figure 9. Astrocytic LTE increases spontaneous TC neuron excitation. **A**, Recordings of membrane potential from neurons in control (left) and after lemniscal afferent-induced LTE (right). SDPs and SDBs (expanded) are indicated by asterisks. I-Clamp, Current clamp; Ctrl, control. **B**, Summarized frequency of SDPs and SDBs in control recordings ($n = 7$ neurons) and after LTE ($n = 5$). **C**, Infrared differential interference contrast image illustrating recording arrangement for a paired TC neuron experiment showing astrocyte (a) and recorded neurons (Neu). **D**, Paired TC neuron recordings after LTE: left, voltage-clamp (VC) recordings showing synchronous SICs; right, current-clamp (IC) comparison showing a synchronous SIC and SDB. **E**, Plots and lines of best fit showing a lack of correlation between SIC amplitudes ($n = 6$) and between SIC amplitude and SDB AP count ($n = 13$) in neuronal pairs. **F**, Voltage recordings from a TC neuron elicited by injection of the acquired SIC waveforms plotted below. **G**, Example of a low-threshold calcium potential (I_T-burst) elicited by step depolarization from -70 mV. **H**, Overlaid SDB AP profile (black) and I_T burst (gray) illustrating contrasting AP frequencies. **I**, Plot of AP interspike interval (ISI) for spontaneous SDBs (black circles) showing similar profile to those elicited by injection of SIC waveforms (white triangles) and their distinct profile compared with I_T bursts (gray squares). **J**, Voltage recording from neuron after LTE showing the blocking effect of ifenprodil (SDPs are asterisked). **K**, Summary of ifenprodil effects on SDP frequency ($n = 9$); **L**, number of APs elicited by SDBs.

iological LTP and behavioral tests that the study used (Agulhon et al., 2010). Our results show that, after the induction of LTE by group I mGluR activation, SICs can be inhibited by intracellular dialysis of the Ca²⁺ chelator BAPTA into local astrocytes, whereas dialysis with control solution has no inhibitory effect. This therefore shows that the glutamate source for SICs is astro-

cytic and that SICs are calcium dependent. SICs were not completely blocked by BAPTA, which most likely indicates that several astrocytes signal to each recorded TC neuron. Indeed, others have found that gliotransmitter signaling effects are dependent on distance from the BAPTA filling electrode (Henneberger et al., 2010). Our findings are therefore consistent with

other studies that find $[Ca^{2+}]_i$-dependent gliotransmitter release (Gómez-Gonzalo et al., 2010; Henneberger et al., 2010; Navarrete and Araque, 2010). The glutamate release mechanism is, however, not clear, and although some groups have found $[Ca^{2+}]_i$-dependent vesicular glutamate release (Bezzi et al., 2004; Jourdain et al., 2007; Perea and Araque, 2007), gliotransmitter release may also be mediated by ion channels, such as volume-regulated anion channels (Kimelberg et al., 2006), or channels that are activated by $[Ca^{2+}]_i$ (Lee et al., 2010).

Extrasynaptic astrocytic signaling

Astrocytic glutamate release has been shown to activate presynaptic (Jourdain et al., 2007), extrasynaptic (Fellin et al., 2004; D'Ascenzo et al., 2007), and synaptic (Lee et al., 2007) NMDA receptors. Comparing the pharmacological sensitivity of synaptically evoked currents in TC neurons with SICs after LTE induction in our study revealed that SICs had a greater sensitivity to the NR2B antagonist ifenprodil. This indicates that SICs target a different NMDA-R population to synaptic glutamate release, and so, by definition, this population must include extrasynaptic receptors. Different subcellular targeting likely indicates different functional consequences. Interestingly, extrasynaptic NR2B-containing receptors have been implicated in mediating cell death signaling (Hardingham et al., 2002) and also in the induction of LTD (Hrabetova et al., 2000). In our study, one potential role presented by the features of LTE is in synaptic plasticity. Because LTE SICs are NMDA-R mediated—notably, NR2B-subunit-containing receptors—it is therefore possible that the SIC-induced calcium signals (Parri et al., 2001) could provide a permissive biochemical intracellular environment for synaptic plasticity when coincident with afferent synaptic input. A putative role in neuronal plasticity in memory may be supported by the gamma range firing elicited in SDBs (Jutras and Buffalo, 2010). In this respect, it may be also significant that LTE SICs can synchronously excite local groups of neurons.

Thalamocortical astrocytic roles

Recordings of astrocytic activity *in vivo* have shown that they respond to sensory input (Wang et al., 2006; Schummers et al., 2008). In somatosensory cortex, astrocytic Ca^{2+} elevations occur in response to whisker deflection (Wang et al., 2006), while in the visual cortex, astrocytes also display direction sensitivity (Schummers et al., 2008). We would therefore predict that, *in vivo*, LTE could be elicited by periods of whisker activation or by thalamocortical loop activity and may indeed be dependent on the patterning of such activity in different arousal states. To influence neuronal activity, however, and contribute to sensory processing, astrocytes must be able to signal to neurons and modify their activity. In contrast to reported astrocyte-mediated excitation to acute synaptic stimulation in hippocampus (Fellin et al., 2004) and nucleus accumbens (D'Ascenzo et al., 2007), LTE of SICs in this regard is significant, because it persists long after afferent activity. This suggests that SDPs could interact with subsequent sensory or corticothalamic inputs to modify thalamic responsiveness.

The generation of SDBs shows that, when the VB thalamus is in "tonic" mode, astrocytes are actually able to generate thalamic activity, which would be expected to drive activity in the thalamocortical loop. The astrocytically derived SDBs are distinctive and distinct from low-threshold calcium (I_T) bursts associated with thalamic delta oscillations and so represent a novel neuronal thalamic activity pattern that may contribute to some observed thalamic and thalamocortical rhythms (Steriade, 2006; Hughes et al., 2008). The frequency of LTE SICs suggests that they may contrib-

ute to infra-slow oscillations such as has been proposed for non-neuronal ATP release in the thalamus (Lörincz et al., 2009). Interestingly, synaptic inputs to the thalamus have been classified in terms of being drivers or modulators depending on their roles and receptor targets (Sherman and Guillery, 1998). Our findings suggest that, in addition to synaptic inputs, thalamic astrocytes may also be considered as thalamic "drivers."

The prevalence of astrocytic mGluR5 expression in different brain areas, however, indicates that LTE could be a general phenomenon, although observations of increased glial-mediated excitation in models of epilepsy (Tian et al., 2005; Fellin et al., 2006b) and pain (Bardoni et al., 2010) also suggest that this mechanism may be recruited under some pathological conditions.

Conclusion

In summary, the findings presented here describe a plasticity of glial–neuron signaling. This plasticity (LTE) is induced by modest continual synaptic activity and can be induced by activity in a single afferent pathway. The persistence of LTE long after the inducing activity suggests that LTE is a form of glial memory of brain activity. Our findings further showed that LTE is a mechanism that generates localized neuronal activity, which may contribute to driving and shaping patterns of thalamocortical loop activity (Steriade, 2006; Hughes et al., 2008).

References

Agulhon C, Fiacco TA, McCarthy KD (2010) Hippocampal short- and long-term plasticity are not modulated by astrocyte Ca^{2+} signaling. Science 327:1250–1254.

Angulo MC, Kozlov AS, Charpak S, Audinat E (2004) Glutamate released from glial cells synchronizes neuronal activity in the hippocampus. J Neurosci 24:6920–6927.

Araque A, Parpura V, Sanzgiri RP, Haydon PG (1999) Tripartite synapses: glia, the unacknowledged partner. Trends Neurosci 22:208–215.

Araque A, Li N, Doyle RT, Haydon PG (2000) SNARE protein-dependent glutamate release from astrocytes. J Neurosci 20:666–673.

Araque A, Martín ED, Perea G, Arellano JI, Buño W (2002) Synaptically released acetylcholine evokes Ca^{2+} elevations in astrocytes in hippocampal slices. J Neurosci 22:2443–2450.

Arsenault D, Zhang ZW (2006) Developmental remodelling of the lemniscal synapse in the ventral basal thalamus of the mouse. J Physiol 573:379–394.

Bardoni R, Ghirri A, Zonta M, Betelli C, Vitale G, Ruggieri V, Sandrini M, Carmignoto G (2010) Glutamate-mediated astrocyte-to-neuron signalling in the rat dorsal horn. J Physiol 588:831–846.

Bezzi P, Gundersen V, Galbete JL, Seifert G, Steinhäuser C, Pilati E, Volterra A (2004) Astrocytes contain a vesicular compartment that is competent for regulated exocytosis of glutamate. Nat Neurosci 7:613–620.

Biber K, Laurie DJ, Berthele A, Sommer B, Tölle TR, Gebicke-Härter PJ, van Calker D, Boddeke HW (1999) Expression and signaling of group I metabotropic glutamate receptors in astrocytes and microglia. J Neurochem 72:1671–1680.

Cornell-Bell AH, Finkbeiner SM, Cooper MS, Smith SJ (1990) Glutamate induces calcium waves in cultured astrocytes: long-range glial signaling. Science 247:470–473.

Crunelli V, Hughes SW (2010) The slow (<1 Hz) rhythm of non-REM sleep: a dialogue between three cardinal oscillators. Nat Neurosci 13:9–17.

Cull-Candy S, Brickley S, Farrant M (2001) NMDA receptor subunits: diversity, development and disease. Curr Opin Neurobiol 11:327–335.

D'Ascenzo M, Fellin T, Terunuma M, Revilla-Sanchez R, Meaney DF, Auberson YP, Moss SJ, Haydon PG (2007) mGluR5 stimulates gliotransmission in the nucleus accumbens. Proc Natl Acad Sci U S A 104:1995–2000.

Daw MI, Scott HL, Isaac JT (2007) Developmental synaptic plasticity at the thalamocortical input to barrel cortex: mechanisms and roles. Mol Cell Neurosci 34:493–502.

Deschênes M, Timofeeva E, Lavallée P (2003) The relay of high-frequency sensory signals in the whisker-to-barreloid pathway. J Neurosci 23:6778–6787.

Fellin T, Pascual O, Gobbo S, Pozzan T, Haydon PG, Carmignoto G (2004)

Neuronal synchrony mediated by astrocytic glutamate through activation of extrasynaptic NMDA receptors. Neuron 43:729–743.

Fellin T, Pozzan T, Carmignoto G (2006a) Purinergic receptors mediate two distinct glutamate release pathways in hippocampal astrocytes. J Biol Chem 281:4274–4284.

Fellin T, Gomez-Gonzalo M, Gobbo S, Carmignoto G, Haydon PG (2006b) Astrocytic glutamate is not necessary for the generation of epileptiform neuronal activity in hippocampal slices. J Neurosci 26:9312–9322.

Fiacco TA, McCarthy KD (2004) Intracellular astrocyte calcium waves in situ increase the frequency of spontaneous AMPA receptor currents in CA1 pyramidal neurons. J Neurosci 24:722–732.

Fiacco TA, Agulhon C, Taves SR, Petravicz J, Casper KB, Dong X, Chen J, McCarthy KD (2007) Selective stimulation of astrocyte calcium in situ does not affect neuronal excitatory synaptic activity. Neuron 54:611–626.

Golshani P, Warren RA, Jones EG (1998) Progression of change in NMDA, non-NMDA, and metabotropic glutamate receptor function at the developing corticothalamic synapse. J Neurophysiol 80:143–154.

Gómez-Gonzalo M, Losi G, Chiavegato A, Zonta M, Cammarota M, Brondi M, Vetri F, Uva L, Pozzan T, de Curtis M, Ratto GM, Carmignoto G (2010) An excitatory loop with astrocytes contributes to drive neurons to seizure threshold. PLoS Biol 8:e1000352.

Hamilton NB, Attwell D (2010) Do astrocytes really exocytose neurotransmitters? Nat Rev Neurosci 11:227–238.

Hardingham GE, Fukunaga Y, Bading H (2002) Extrasynaptic NMDARs oppose synaptic NMDARs by triggering CREB shut-off and cell death pathways. Nat Neurosci 5:405–414.

Henneberger C, Papouin T, Oliet SH, Rusakov DA (2010) Long-term potentiation depends on release of D-serine from astrocytes. Nature 463:232–236.

Hrabetova S, Serrano P, Blace N, Tse HW, Skifter DA, Jane DE, Monaghan DT, Sacktor TC (2000) Distinct NMDA receptor subpopulations contribute to long-term potentiation and long-term depression induction. J Neurosci 20:RC81(1–6).

Hughes SW, Cope DW, Blethyn KL, Crunelli V (2002) Cellular mechanisms of the slow (<1 Hz) oscillation in thalamocortical neurons in vitro. Neuron 33:947–958.

Hughes SW, Errington A, Lorincz ML, Kékesi KA, Juhász G, Orbán G, Cope DW, Crunelli V (2008) Novel modes of rhythmic burst firing at cognitively-relevant frequencies in thalamocortical neurons. Brain Res 1235:12–20.

Ivy GO, Killackey HP (1982) Ontogenetic changes in the projections of neocortical neurons. J Neurosci 2:735–743.

Jahnsen H, Llinás R (1984) Electrophysiological properties of guinea-pig thalamic neurones: an in vitro study. J Physiol 349:205–226.

Jourdain P, Bergersen LH, Bhaukaurally K, Bezzi P, Santello M, Domercq M, Matute C, Tonello F, Gundersen V, Volterra A (2007) Glutamate exocytosis from astrocytes controls synaptic strength. Nat Neurosci 10: 331–339.

Jutras MJ, Buffalo EA (2010) Synchronous neural activity and memory formation. Curr Opin Neurobiol 20:150–155.

Kafitz KW, Meier SD, Stephan J, Rose CR (2008) Developmental profile and properties of sulforhodamine 101-labeled glial cells in acute brain slices of rat hippocampus. J Neurosci Methods 169:84–92.

Kang J, Jiang L, Goldman SA, Nedergaard M (1998) Astrocyte-mediated potentiation of inhibitory synaptic transmission. Nat Neurosci 1:683–692.

Kimelberg HK, Macvicar BA, Sontheimer H (2006) Anion channels in astrocytes: biophysics, pharmacology, and function. Glia 54:747–757.

Lalo U, Pankratov Y, Kirchhoff F, North RA, Verkhratsky A (2006) NMDA receptors mediate neuron-to-glia signaling in mouse cortical astrocytes. J Neurosci 26:2673–2683.

Landisman CE, Connors BW (2005) Long-term modulation of electrical synapses in the mammalian thalamus. Science 310:1809–1813.

Lee CJ, Mannaioni G, Yuan H, Woo DH, Gingrich MB, Traynelis SF (2007) Astrocytic control of synaptic NMDA receptors. J Physiol 581:1057–1081.

Lee S, Yoon BE, Berglund K, Oh SJ, Park H, Shin HS, Augustine GJ, Lee CJ (2010) Channel-mediated tonic GABA release from glia. Science 330: 790–796.

Liu QS, Xu Q, Kang J, Nedergaard M (2004a) Astrocyte activation of presynaptic metabotropic glutamate receptors modulates hippocampal inhibitory synaptic transmission. Neuron Glia Biol 1:307–316.

Liu XB, Murray KD, Jones EG (2004b) Switching of NMDA receptor 2A and 2B subunits at thalamic and cortical synapses during early postnatal development. J Neurosci 24:8885–8895.

Lörincz ML, Geall F, Bao Y, Crunelli V, Hughes SW (2009) ATP-dependent infra-slow (<0.1 Hz) oscillations in thalamic networks. PLoS One 4:e4447.

Malenka RC, Nicoll RA (1993) NMDA-receptor-dependent synaptic plasticity: multiple forms and mechanisms. Trends Neurosci 16:521–527.

Matthews MA, Narayanan CH, Narayanan Y, Onge MF (1977) Neuronal maturation and synaptogenesis in the rat ventrobasal complex: alignment with developmental changes in rate and severity of axon reaction. J Comp Neurol 173:745–772.

Navarrete M, Araque A (2010) Endocannabinoids potentiate synaptic transmission through stimulation of astrocytes. Neuron 68:113–126.

Oliet SH, Piet R, Poulain DA (2001) Control of glutamate clearance and synaptic efficacy by glial coverage of neurons. Science 292:923–926.

Panatier A, Theodosis DT, Mothet JP, Touquet B, Pollegioni L, Poulain DA, Oliet SH (2006) Glia-derived D-serine controls NMDA receptor activity and synaptic memory. Cell 125:775–784.

Parri HR, Crunelli V (2001) Pacemaker calcium oscillations in thalamic astrocytes in situ. Neuroreport 12:3897–3900.

Parri HR, Crunelli V (2002) Astrocytes, spontaneity, and the developing thalamus. J Physiol Paris 96:221–230.

Parri HR, Crunelli V (2003) The role of Ca2+ in the generation of spontaneous astrocytic Ca^{2+} oscillations. Neuroscience 120:979–992.

Parri HR, Gould TM, Crunelli V (2001) Spontaneous astrocytic Ca^{2+} oscillations in situ drive NMDAR-mediated neuronal excitation. Nat Neurosci 4:803–812.

Parri HR, Gould TM, Crunelli V (2010) Sensory and cortical activation of distinct glial cell subtypes in the somatosensory thalamus of young rats. Eur J Neurosci 32:29–40.

Pascual O, Casper KB, Kubera C, Zhang J, Revilla-Sanchez R, Sul JY, Takano H, Moss SJ, McCarthy K, Haydon PG (2005) Astrocytic purinergic signaling coordinates synaptic networks. Science 310:113–116.

Pasti L, Volterra A, Pozzan T, Carmignoto G (1997) Intracellular calcium oscillations in astrocytes: a highly plastic, bidirectional form of communication between neurons and astrocytes *in situ*. J Neurosci 17:7817–7830.

Perea G, Araque A (2005) Properties of synaptically evoked astrocyte calcium signal reveal synaptic information processing by astrocytes. J Neurosci 25:2192–2203.

Perea G, Araque A (2007) Astrocytes potentiate transmitter release at single hippocampal synapses. Science 317:1083–1086.

Petravicz J, Fiacco TA, McCarthy KD (2008) Loss of IP3 receptor-dependent Ca^{2+} increases in hippocampal astrocytes does not affect baseline CA1 pyramidal neuron synaptic activity. J Neurosci 28:4967–4973.

Porter JT, McCarthy KD (1996) Hippocampal astrocytes in situ respond to glutamate released from synaptic terminals. J Neurosci 16:5073–5081.

Redman S (1990) Quantal analysis of synaptic potentials in neurons of the central nervous system. Physiol Rev 70:165–198.

Schummers J, Yu H, Sur M (2008) Tuned responses of astrocytes and their influence on hemodynamic signals in the visual cortex. Science 320: 1638–1643.

Serrano A, Haddjeri N, Lacaille JC, Robitaille R (2006) GABAergic network activation of glial cells underlies hippocampal heterosynaptic depression. J Neurosci 26:5370–5382.

Sherman SM (2001) Tonic and burst firing: dual modes of thalamocortical relay. Trends Neurosci 24:122–126.

Sherman SM, Guillery RW (1998) On the actions that one nerve cell can have on another: distinguishing "drivers" from "modulators." Proc Natl Acad Sci U S A 95:7121–7126.

Steriade M (2006) Grouping of brain rhythms in corticothalamic systems. Neuroscience 137:1087–1106.

Tian GF, Azmi H, Takano T, Xu Q, Peng W, Lin J, Oberheim N, Lou N, Wang X, Zielke HR, Kang J, Nedergaard M (2005) An astrocytic basis of epilepsy. Nat Med 11:973–981.

Volterra A, Meldolesi J (2005) Astrocytes, from brain glue to communication elements: the revolution continues. Nat Rev Neurosci 6:626–640.

Wang X, Lou N, Xu Q, Tian GF, Peng WG, Han X, Kang J, Takano T, Nedergaard M (2006) Astrocytic Ca^{2+} signaling evoked by sensory stimulation in vivo. Nat Neurosci 9:816–823.

Yang Y, Ge W, Chen Y, Zhang Z, Shen W, Wu C, Poo M, Duan S (2003) Contribution of astrocytes to hippocampal long-term potentiation through release of D-serine. Proc Natl Acad Sci U S A 100:15194–15199.